Photoisomerization and Photochemistry of Matrix-Isolated 3-Furaldehyde

Nihal Kuş,[*,†,‡] **Igor Reva,**[‡] **and Rui Fausto**[‡]

Department of Physics, Anadolu University, 26470 Eskişehir, Turkey, and Department of Chemistry, University of Coimbra, 3004-535 Coimbra, Portugal

3-Furaldehyde (3FA) was isolated in an argon matrix at 12 K and studied using FTIR spectroscopy and quantum chemistry. The molecule has two conformers, with trans and cis orientation of the O=C−C=C dihedral angle. At the B3LYP/6-311++G(d,p) level of theory, the trans form was computed to be ca. 4 kJ mol^{-1} more stable than the cis form. The relative stability of the two conformers was explained using the natural bond orbital (NBO) method. In fair agreement with their calculated relative energies and the high barrier of rotamerization (ca. 34 kJ mol^{-1} from trans to cis), the trans and cis conformers were trapped in an argon matrix from the compound room temperature gas phase in proportion ∼7:1. The experimentally observed vibrational signatures of the two forms are in a good agreement with the theoretically calculated spectra. Broad-band UV-irradiation ($\lambda > 234$ nm) of the matrix-isolated compound resulted in partial trans → cis isomerization, which ended at a photostationary state with the trans/cis ratio being ca. 1.85:1. This result was interpreted based on results of time-dependent DFT calculations. Irradiation at higher energies ($\lambda > 200$ nm) led to decarbonylation of the compound, yielding furan, cyclopropene-3-carbaldehyde, and two C_3H_4 isomers: cyclopropene and propadiene.

Introduction

Furans are five-membered aromatic heterocyclic rings formed by one oxygen and four carbon atoms. These organic compounds play important roles in the pharmaceutical and chemical industries. Volatile furans, like methylfurans and furaldehydes, are important atmospheric pollutants resulting from biomass burning and are produced, for example, as a result of forest fires.[1,2] A wide range of furan derivatives has been found to be hazardous to both animals and human beings, with the polychlorinated furans being among the most toxic volatile substances known.[3−5] The presence of potentially toxic compounds (such as reactive aldehydes) in foods has been attracting increasing attention ever since consumer protection and quality control gained importance. For example, furanic aldehydes were reported to be present in honey[6] and popped popcorn.[7]

3-Furaldehyde (3FA) is among the furan pollutants found in atmosphere, and the investigation of its structure and chemical reactivity may contribute to assess the atmospheric reactivity of such compounds and to elucidate their final fates in the atmosphere.[8] The study of the possible photodegradation processes of the compound, under well-controlled laboratorial conditions, appears particularly relevant to attain such goals.

The first synthetic procedure to obtain 3FA was reported as early as in 1932.[9] 3FA, as well as its structural isomer 2-furaldehyde (2FA; also known as furfural), have been the subject of many experimental and theoretical studies in the 1970s and 1980s.[10−20] 3FA and 2FA have been found to exist in the gas phase, nematic and isotropic solutions, and neat liquid state, as a mixture of two planar conformers differing by rotation of the aldehyde group around the exocyclic C−C bond (cis and trans with respect to the ring oxygen atom; see Scheme 1).[21−28] For 2FA, the trans conformer was found to be the lowest energy

SCHEME 1: Conformers of 3-Furaldehyde and Adopted Atom Numbering
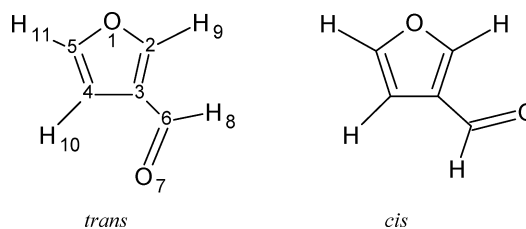
form, with gas phase reported values for $\Delta E_{(cis-trans)}$ ranging from 3.10 to 8.79 kJ mol^{-1},[18−27] which implies a minimum expected population of the conformational ground state of 2FA at room temperature (RT) of ca. 80%.

For 3FA, similarly to 2FA, all the reports indicate that the trans structure (regarding the C=C−C=O dihedral angle) is the most stable conformer. On the basis of the study of the microwave spectrum, Marstokk and Møllendal showed that the trans conformer of 3FA is at least 5 kJ mol^{-1} more stable than any other rotameric form of this molecule,[29] that is, should contribute to the equilibrium population at RT with at least 88%. Liégeois et al. studied the rotational isomerism in 3FA through dipole moment thermal variation and found that about 70% of 3FA exist in the trans form.[30] Benassi et al. undertook a conformational analysis in formyl derivatives of furan via measurements of the long-range $^{13}C^1H$ spin−spin coupling constants.[15] They found that for the 3-formyl derivatives (including 3FA) the conformational equilibrium was significantly dependent on solvent polarity, with the amount of trans form, prevailing in the equilibrium mixture, increasing with solvent polarity. They reported that the minor 3FA cis conformer population depends on the polarity of the solvent ranging from 6% in nonpolar solvents (e.g., cyclohexane), down to 3% in chloroform and, further, to 0% in DMSO. The thermodynamic aspects of these equilibria were discussed and, by employing

* To whom correspondence should be addressed. E-mail: nkus@anadolu.edu.tr.
† Anadolu University.
‡ University of Coimbra.

classical reaction-field theory, it was tentatively shown that the increase of the less polar trans form of 3FA in polar media should be due to the fact that quadrupolar contributions prevail over dipolar effects.[15] Lunazzi et al. studied conformations of 3FA by dynamic NMR and predicted that the proportion of the minor conformer should be about 11% at RT.[31] The preferential conformations of 3FA were also determined by use of simulated lanthanide induced shifts.[32] The ratio of the two rotamers was found to be similar as obtained by other NMR methods, and the trans conformation of the aldehyde group was found to dominate.

Vibrational spectra of 3FA were studied mainly in condensed phases in the region of the carbonyl stretching vibration.[14,17,29] These studies have also indicated the existence of two planar conformers differing by internal rotation of the aldehyde group. The experimental observation of these two conformers has been reported by Volka et al.,[17] through the analysis of the aldehyde C−H and C=O stretching regions of the infrared spectra of the compound and some of its isotopomers in the gas phase and in CCl$_4$ solution.

To the best of our knowledge, no data have been reported hitherto on the full mid-infrared experimental spectra of 3FA, nor about the photochemistry of neat 3FA. In the present investigation, 3FA was isolated in cryogenic (12 K) inert matrices, and its structure, spectroscopic properties and photochemical behavior were studied using infrared spectroscopy, supported by high level quantum chemical calculations.

Experimental and Computational Methods

Matrix Isolation FTIR and Photochemical Experiments. A commercial sample of 3-furaldehyde (Aldrich, 98%) was placed in a Knudsen cell[33] connected to the vacuum chamber of the cryostat. Room-temperature vapor of the compound was deposited, together with a large excess of argon (N60, Air Liquide), onto the optical CsI substrate of the cryostat, cooled to 12 K by an APD Cryogenics DE-202A closed-cycle refrigerator system. Before cooling down the cryostat, the vapors over the compound in the Knudsen cell were pumped out several times, in order to remove possible traces of volatile impurities from the sample.

Infrared spectra were collected with 0.5 cm^{-1} resolution using a Nicolet 6700 FTIR spectrometer, equipped with a DTGS detector and a KBr beam splitter. The instrument was purged by a stream of dry air to remove water and CO$_2$ vapors.

The matrices were irradiated using different cutoff filters (transmitting light with $\lambda > 375$, 337, 283, 234 nm) or directly through the outer quartz window of the cryostat (transmitting light with $\lambda > 200$ nm) using a 300 W output power of the 500 W Hg(Xe) arc lamp (Oriel, Newport). To prevent overheating of the matrix, the arc lamp was equipped with 8 cm water filter in all irradiations.

Theoretical Calculations. All quantum chemical calculations were performed with Gaussian 03 (revision C.02).[34] The equilibrium geometries for all studied species were fully optimized at the DFT level of theory with the standard 6-311++G(d,p) basis set.[35,36] The DFT calculations were carried out with the three-parameter density functional (B3LYP), which includes Becke's gradient exchange correction,[37] and the Lee, Young, and Parr correlation functional.[38] The geometry optimizations were followed by infrared (IR) spectra calculations, which also allowed characterization of the nature of the stationary point through inspection of the corresponding Hessian matrix. Energies of the low-energy excited states were calculated using the time-dependent density functional theory (TD-DFT)[39,40]
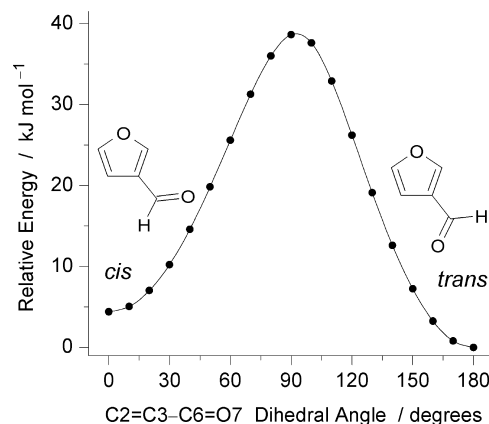

Figure 1. B3LYP/6-311++G(d,p) calculated potential energy profile for conformational interconversion in 3FA.

at the B3LYP/6-311++G(d,p) level. Natural bond orbital (NBO) analysis was performed according to Weinhold and co-workers,[41,42] using NBO 3 as implemented in Gaussian 03.

The theoretical normal modes were analyzed by carrying out the potential energy distribution (PED) calculations. Transformations of the theoretical B3LYP/6-311++G(d,p) force constants calculated with respect to the Cartesian coordinates to the force constants with respect to the molecule fixed internal coordinates allowed the PED analysis to be carried out as described by Schachtschneider and Mortimer.[43] The internal symmetry coordinates used in this analysis were defined as recommended by Pulay et al.[44]

Results and Discussion

Geometries and Relative Stability of 3FA Conformers. Scheme 1 shows the geometries of the trans and cis conformers of 3FA, together with the adopted atom numbering. Both conformers have a planar geometry (C_s point group). The calculated optimized bond lengths and angles for the two conformers are provided in Table S1 (Supporting Information).

According to the calculations, the trans conformer is more stable than the cis form by 4.40 kJ mol^{-1} (4.03 kJ mol^{-1}, if zero point vibrational energy correction is taken into account). The calculated difference in free energy between the conformers at RT (298.15 K) is 3.83 kJ mol^{-1}, thus leading to an expected trans/cis gas phase equilibrium population ratio at RT of ~4.6: 1 (82% trans, 18% cis).

The calculated energy barrier for trans → cis isomerization in 3FA, by internal rotation of the aldehyde group about the exocyclic C3−C6 bond (Figure 1), was found to be 38.8 kJ mol^{-1} (34.4 kJ mol^{-1} in the reverse direction; these values change to 36.8 and 32.8 kJ mol^{-1} if zero-point corrections are included). The corresponding free energy of activation at RT is 38.1 kJ mol^{-1} (34.3 kJ mol^{-1} for the reverse process). These findings are in agreement with the calculated value of about 38 kJ mol^{-1} and experimental value of 34.7 kJ mol^{-1} reported for this barrier in the literature.[16,31]

The relative energy of the two conformers of 3FA as well as the barrier to conformational isomerization can be also compared with those reported for similar molecules. For instance, in 2-furaldehyde (2FA) calculations performed by Ashish and Ramasami[21] at the same level of theory as those reported in the present study yield $\Delta E_{(cis-trans)} = 3.10$ kJ mol^{-1} and $\Delta E_{(trans \rightarrow cis)} = 51.7$ kJ mol^{-1}. The higher barrier found in 2FA compared to 3FA indicates a higher degree of double bond character in the C−C exocyclic linkage for the first compound. In agreement
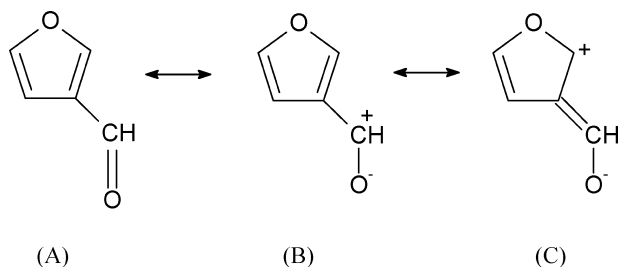
Photoisomerization and Photochemistry of 3-Furaldehyde

J. Phys. Chem. A, Vol. 114, No. 47, 2010 **12429**

Figure 2. Resonance structures showing the mesomerism involving the furan ring and the aldehyde substituent.

with this interpretation, the exocyclic C−C bond length was found to be significantly shorter in 2FA (1.455 Å in both trans and cis conformers)[21] compared to 3FA (trans: 1.462 Å; cis: 1.465 Å; see Table S1 in the Supporting Information). In the analogues of 2FA having the aldehyde oxygen atom replaced by a sulfur or a selenium atom, $\Delta E_{\text{(cis−trans)}}$ and $\Delta E_{\text{(trans→cis)}}$ were calculated at the same level of theory as being 2.96 and 60.7 kJ mol^{-1} (for the S-substituted compound) and 2.76 and 63.9 kJ mol^{-1} (Se).[21] The increase in the isomerization barrier along the series O, S, Se indicates that, besides π-system conjugative effects, other factors such as hyperconjugation, dispersive forces, and electrostatic interactions must also influence the energy barrier. On the other hand, the reduction in $\Delta E_{\text{(cis−trans)}}$ along the series O, S, Se can be correlated with the progressive lack of importance along this series of the repulsive interaction between the nearly parallel bond-dipoles associated with the C=X (X = O, S, Se) bond and the closest located endocyclic C−O bond in the cis conformer. Very interestingly, introduction of substituents in the furan ring of 2FA does not influence much the $\Delta E_{\text{(cis−trans)}}$ and $\Delta E_{\text{(trans→cis)}}$ values, except when performed in the ortho position to the aldehyde group,[22] revealing the importance of the vicinal interactions in this type of molecules.

Simple examination of the structures of the two conformers of 3FA allows to conclude that steric interactions in both forms have to be practically identical. The aldehyde group in 3FA has a negative inductive effect, withdrawing electronic charge from the aromatic ring through the σ-system, and, what is more important, a negative mesomeric effect withdrawing electronic charge from the aromatic ring through the π-system. According to the resonance structures shown in Figure 2, one can then expect that the charge on C2 is considerably more positive than on C4. This effect can then be expected to strongly reduce the polarity of the C2−H9 comparatively to that of the C4−H10 bond. Such difference in the polarity of these bonds is, as described below, the key property leading to the greater stability of the trans conformer compared to the cis form.

In order to evaluate the reasons for the greater stability of the trans conformer in 3FA, compared to the cis conformer, a detailed analysis of the electronic structure of the two forms was carried out by examining the orbital interactions in the two conformers, with help of the natural bond orbital (NBO) method.

The NBO charges for the two conformers are shown in Table 1. The general trends regarding the charges on atoms in both conformers are identical. As anticipated, the C4−H10 bond is considerably polarized in both conformers, whereas the C2−H9 bond is practically nonpolarized. For example in the trans conformer, the charges on C4 and H10 are −0.264 and +0.241 e, whereas those on C2 and H9 are +0.191 and +0.203 e. The interaction between the dipoles associated with the highly polarized C=O bond of the aldehyde substituent (charges on C6 and O7 are, in both conformers, of ca. +0.41 and −0.53 e, respectively) and the C4−H10 bond is then the main stabilizing

TABLE 1: Natural Bond Orbital (NBO) Atomic Charges^a in Trans and Cis Conformers of 3FA, Obtained from B3LYP/ 6-311++G(d,p) Calculations^b

atom	NBO charges	
	trans	cis
O1	−0.446	−0.440
C2	0.191	0.211
C3	−0.242	−0.255
C4	−0.264	−0.274
C5	0.127	0.123
C6	0.410	0.416
O7	−0.530	−0.531
H8	0.108	0.107
H9	0.203	0.212
H10	0.241	0.228
H11	0.202	0.202

^{a} In units of electron; $e = 1.60217646 \times 10^{-19}$ C. ^{b} See Figure 1 for atom numbering.

interaction justifying the lower energy of the trans compared to the cis conformer. In the latter conformer, the C=O bond is facing the practically nonpolarized C2−H9 bond.

Calculated NBOs having a significant occupancy are presented in Tables S2 and S3 (Supporting Information), for trans- and cis-3FA, respectively. The description is made in the space of input atomic orbitals [as given by the 6-311++G(d,p) basis set used in the calculations]. These tables also show the percentage ratio (extracted from the NBO polarization coefficients) of the atomic orbitals on each atom forming a bond, for the NBO orbitals. The NBO analysis supports the idea of a greater polarization of the C4−H10 bond compared to the C2−H9 bond extracted from the NBO charges analysis presented above.

Regarding the carbonyl bond in the two conformers, the NBO analysis reveals the following features: (i) the $\sigma(C=O)$ bonding orbital is, as expected, strongly polarized toward the oxygen atom, the occupancies being nearly equal in the two conformers, (ii) the $\pi(C=O)$ bonding orbital is even more polarized toward the oxygen atom, but in this case the occupancy is slightly larger in the trans conformer (1.979 e, vs 1.971 e in the cis form), as it could be expected considering the relevance of the C=O/ C4−H10 bond-dipole interaction in the trans isomer; (iii) the $\sigma^*(C=O)$ and $\pi^*(C=O)$ antibonding orbitals are polarized toward the carbon atom, the occupancy of the $\pi^*(C=O)$ antibonding orbitals in both conformers being considerably large (0.123 and 0.117 e, in trans and cis conformers, respectively).

The C5−O1−C2 linkage was also found to present some interesting characteristics. According to the NBO results, the ring oxygen atom is hybridized sp^2, with the two hybrid orbitals involved in the C5−O1 and C2−O1 bonds exhibiting a strong polarization toward the oxygen atom and having an increased p character. In turn, the third hybrid orbital, which corresponds to a lone-electron pair (lp) orbital, has a reduced p character (see Tables S2 and S3 of the Supporting Information). The second lp orbital exhibits pure p character, which favors the π delocalization within the furan ring. In agreement with the interpretation based on the NBO atomic charges (see Table 1), the obtained NBO coefficients show that the polarization of the O1−C2 bond is greater in the case of the cis than in the trans conformer. On the other hand, one can see that the polarization of the O1−C5 bond is greater in the trans conformer.

The most relevant NBO interactions for both isomers are listed in Table 2 and plotted in Figure 3. Orbital interaction energies, $E(2)$, between filled (donor) and empty (acceptor)

TABLE 2: Stabilization Energies for Selected NBO Pairs as Given by Second-Order Perturbation Theory Analysis of the Fock Matrix in the NBO Basis for 3FA (Conformers Cis and Trans) Obtained from the B3LYP/6-311++G(d,p) Calculations[a]

pair name	donor NBO	acceptor NBO	$E(2)$ (kJ mol^{-1})	
			trans	cis
A	π (C2−C3)	π* (C4−C5)	67.40	72.40
B	π (C2−C3)	π* (C6−O7)	87.49	82.51
C	π (C4−C5)	π* (C2−C3)	63.39	61.34
D	LP2 (O1)	π* (C2−C3)	126.27	128.41
E	LP2 (O1)	π* (C4−C5)	97.19	101.00
F	LP2 (O7)	σ* (C3−C6)	72.25	73.01
G	LP2 (O7)	σ* (C6−H8)	96.06	95.35

[a] See atom numbering in Figure 1. LP, lone electron pair orbital.

NBOs (including non-Lewis extra-valence Rydberg orbitals) are obtained from the second-order perturbation approach,[42]

$$E(2) = \Delta E_{ij} - q_i \frac{F_{ij}^2}{\varepsilon_j - \varepsilon_i}$$

where F_{ij}^2 is the Fock matrix element between the i and j NBO orbitals; ε_j and ε_i are the energies of the acceptor and donor NBOs; and q_i is the occupancy of the donor orbital.

As shown in Table 2, the most important NBO interactions in both 3FA conformers are of the same type, and their relative importance is also similar. In relation with interactions involving the π-system of the molecule, orbital interactions of types A and C in Table 2 reflect the delocalization over the carbon atoms of the furan ring, those of types D and E, between the lone
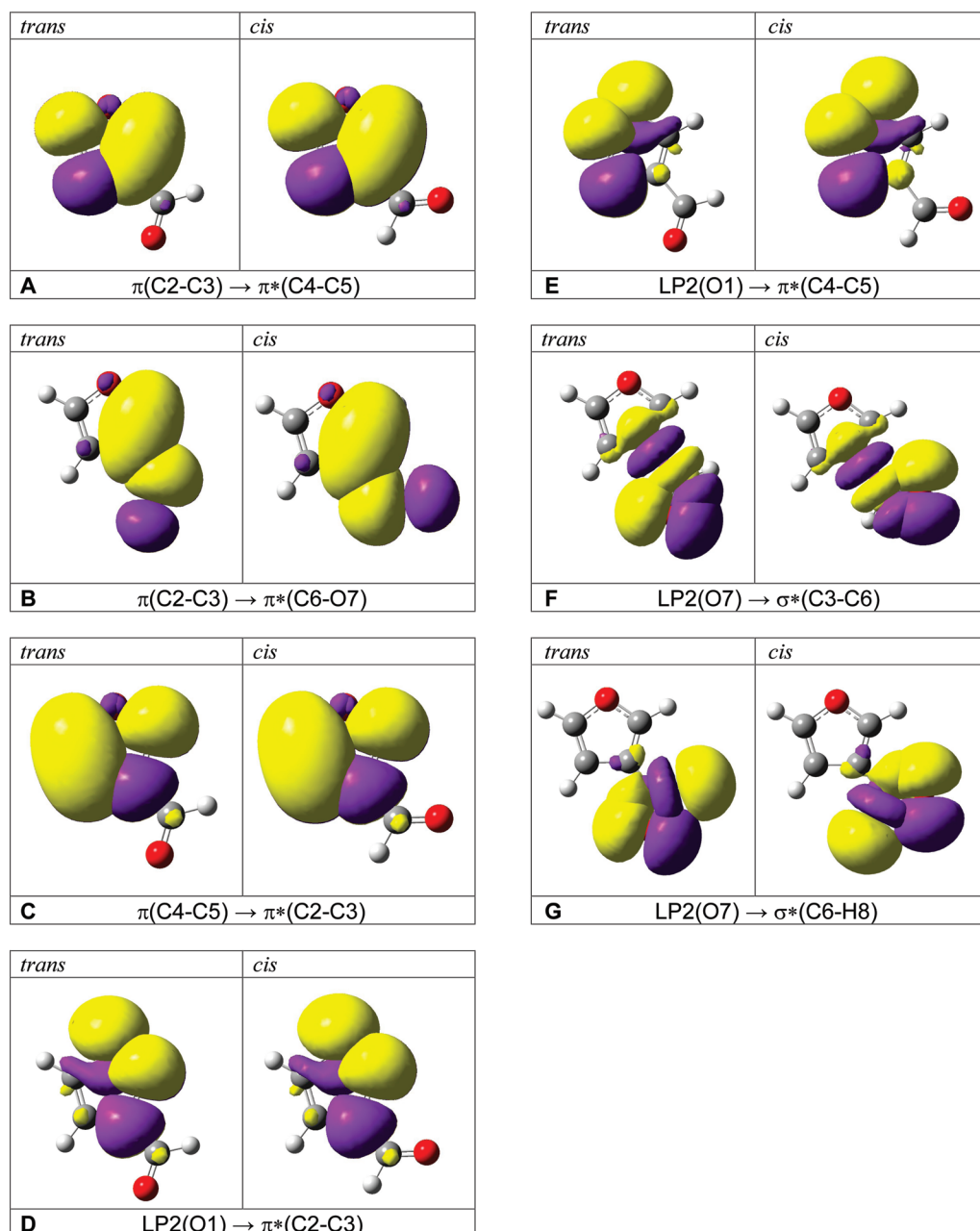

Figure 3. Electron density surfaces of selected NBOs for trans and cis conformers of 3FA calculated at the B3LYP/6-311++G(d,p) level of theory showing the dominant orbital interactions (see Table 2). Isovalues of the electron densities are equal to 0.02 e. Yellow and violet colors correspond to negative and positive wave function signs. Color codes for atoms: red, O; gray, C; white, H.

Photoisomerization and Photochemistry of 3-Furaldehyde

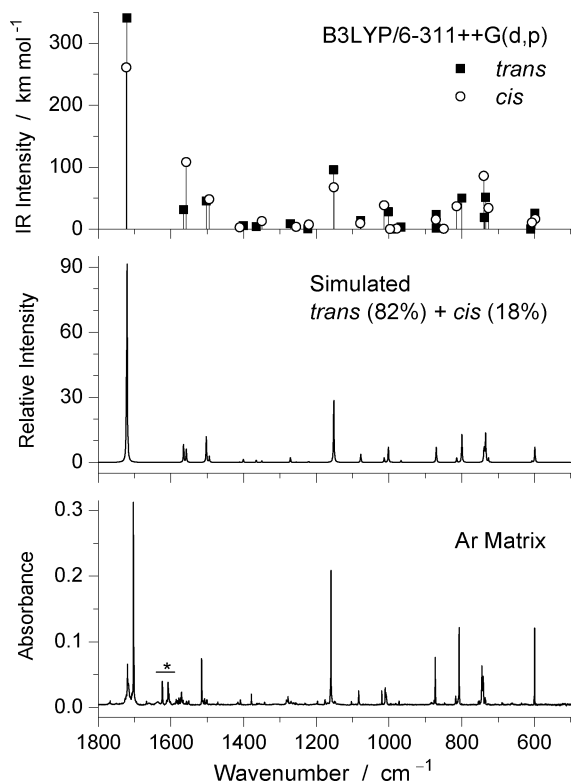*J. Phys. Chem. A, Vol. 114, No. 47, 2010* **12431**

Figure 4. Infrared spectra of 3FA. From bottom to top: spectrum of the matrix-isolated compound (argon matrix, 12 K; initial vapor at room temperature); simulated spectrum based on the B3LYP/6-311++G(d,p) calculated infrared spectra of trans and cis conformers weighted by their predicted relative populations in gas phase at room temperature (82% trans; 18% cis); calculated spectra for trans and cis conformers. The simulated spectrum was obtained using Lorentzian functions centered at the calculated wavenumbers (scaled by 0.978) using the full widths at half-maximum-height (fwhm) equal to 2 cm^{-1}. In the experimental spectrum, bands of monomeric water impurity present in the matrix are indicated by an asterisk.
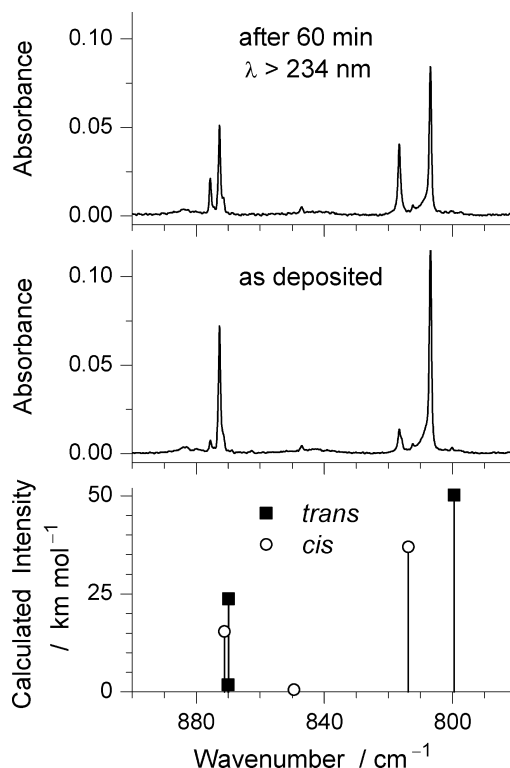

Figure 5. Bottom: Fragment of the theoretical infrared spectra of trans (squares) and cis (circles) conformers of 3FA, calculated at the B3LYP/6-311++G(d,p) level (wavenumbers scaled by 0.978). Middle: Fragment of the experimental spectrum of 3FA isolated in a freshly deposited argon matrix. Top: Experimental spectrum of the same sample after 60 min of UV-irradiation ($\lambda > 234$ nm).

electron pair of the furan oxygen atom and the carbon ring atoms and, finally, that of type B, between the C2−C3 bond of the furan ring and the carbonyl group (see also Figure 3). On the whole, these interactions point to a slightly larger importance of the mesomeric structures B and C (see Figure 2) in cis than in trans 3FA (sum $E(2)$ resulting from the main π-type orbital interactions in trans and cis are 441.7 and 445.7 kJ mol^{-1}, respectively). On the other hand, the main σ-type NBO interactions (F and G in Table 2) are identically important in both conformers (sum σ-type E(2) is 168.3 kJ mol^{-1} in both conformers). These interactions correlate with the electronic charge back-donation from the aldehyde oxygen lone electron pairs (specifically the p-type lone pair; LP2) to the C3−C6 bond and, in particular, to the C6−H8 aldehyde bond. This back-donation effect is well-known and has been described long ago as the most important effect leading to the observed elongation of a C−H bond connected to a carbonyl moiety as well as to its reduced C−H stretching frequency (e.g., in aldehydes and formic acid derivatives).[45−47]

The calculated total stabilization energy associated with the main orbital interactions favors the cis conformer by ca. 4 kJ mol^{-1} over the trans form, implying that, globally, the less important orbital interactions and other type of stabilizing effects not evaluated by the NBO analysis, in particular the above-mentioned dipolar interaction between the C=O and C4−H10 bond dipoles in the trans conformer, must account for ca. 8 kJ mol^{-1} in favor of the trans conformer.

Matrix Isolation Infrared Spectra and Conformational Photoisomerism in 3FA. 3FA has 27 fundamental vibrations, spanning the irreducible representations 19A′ + 8A″ in both trans and cis conformers. According to the selection rules, all modes are active in the infrared. The B3LYP/6-311++G(d,p) calculated infrared spectra for the two conformers and results of normal coordinate analysis are provided in the Supporting Information (Tables S4−S6). Figure 4 shows the infrared spectrum of 3FA isolated in an argon matrix ($T = 12$ K; 1800−500 cm^{-1} frequency range), together with the calculated spectra for trans and cis conformers (in the form of stick spectra), and the simulated theoretical spectrum obtained by adding the calculated spectra of the two conformers weighted by their expected relative populations in gas phase at room temperature (82% trans, 18% cis).

As seen in Figure 4, the simulated spectrum nicely fits the experimental one. Although calculation of the relative population of the two conformers present in the as-deposited matrix, based on band intensities, yielded a slightly larger trans/cis population ratio (7.3, i.e., 88%:12%) compared to that predicted theoretically (4.6, i.e., 82%:18%), one can say that the two conformers of 3FA could be efficiently trapped in the matrix. These results confirm the adequate description by the calculations of the potential energy surface landscape of the molecule in the gas phase, in particular this is in agreement with the theoretically calculated high energy barrier for conformational isomerization in 3FA (>32 kJ mol^{-1}; see previous section). It should be additionally noted that the conformational trans/cis ratio of 88%:12%, deduced from the present matrix-isolation experiment, corresponds to the equilibrium mixture (at room temperature) of two conformers that have the free energy difference of ca. 5 kJ mol^{-1}. This estimate is in a good agreement with the

TABLE 3: Assignments of Observed Infrared Bands to Trans and Cis Conformers of 3FA[a]

assignment	symmetry	observed (Ar matrix)[b] trans	cis	calculated B3LYP/6-311++G(d,p)[c] trans		cis	
ν(C−H10/11)$_s$	A'	n.obs.	n.obs.	3214.0	(0.05)	3214.6	(1.0)
ν(C−H9)	A'	n.obs.	n.obs.	3194.6	(1.4)	3209.3	(3.6)
ν(C−H10/11)$_{as}$	A'	3144.9	n.obs.	3188.6	(2.9)	3173.6	(0.9)
ν(C−H8)	A'	2840.2	2855.7	2832.6	(109.5)	2835.2	(116.4)
ν(C=O)	A'	1703.2	1711.4	1721.0	(340.5)	1722.7	(261.2)
			1707.8				
			1705.4				
ν ring3	A'	1577.8	1573.0	1565.3	(31.6)	1557.8	(108.2)
		1570.9	1566.7				
ν ring4	A'	1515.5	1507.3	1502.8	(45.7)	1494.5	(48.1)
δ(C−H8)	A'	1408.8	1419.8	1401.1	(5.6)	1411.0	(2.7)
ν ring1	A'	1378.6	1363.8	1365.5	(4.0)	1350.0	(12.9)
			1356.9				
δ(C−H11)	A'	1282.2	1231.4	1271.4	(8.7)	1220.6	(7.4)
		1280.2					
		1277.8					
δ(C−H9)	A'	n.obs.	1263.6	1223.3	(0.6)	1255.5	(3.7)
ν ring2	A'	1159.8	1159.2	1152.1	(95.9)	1151.9	(67.5)
δ(C−H10)	A'	1083.7	1085.6	1077.6	(13.8)	1079.0	(9.8)
ν ring5	A'	1010.4	1019.9	1001.8	(28.1)	1013.4	(38.6)
		1008.5					
		1007.1					
γ(C−H8)	A''	995.4(?)	n.obs.	992.1	(0.3)	997.2	(0.1)
δ ring2	A'	972.5	987.0(?)	966.9	(3.4)	978.4	(0.8)
δ ring1	A'	871.6	875.6	870.0	(1.8)	871.2	(15.4)
γ(C−H10/11)$_{as}$	A''	872.7	847.1	869.9	(23.7)	849.4	(0.5)
γ(C−H9)	A''	806.8	816.6	799.5	(50.2)	813.7	(37.0)
γ(C−H10/11)$_s$	A''	744.5	736.2	737.5	(19.0)	726.3	(34.1)
			735.3				
δ(C=O)	A'	741.2	~742.6	734.2	(51.5)	739.3	(85.8)
τ ring1	A''	n.obs.	600.4	609.8	(0.0004)	597.8	(16.3)
τ ring2	A''	599.0	600.4	598.7	(25.6)	606.6	(10.8)
ν(C6−C3)	A'	n.obs.	n.obs.	481.6	(0.6)	475.5	(0.2)
γ(C6−C3)	A''	n.i.	n.i.	275.5	(9.3)	242.8	(5.2)
δ(C6−C3)	A'	n.i.	n.i.	193.2	(11.6)	195.7	(5.3)
τ(C6−C3)	A''	n.i.	n.i.	133.6	(6.8)	129.5	(6.9)

[a] Wavenumbers in cm^{-1}. ν, stretching; δ, bending; γ, rocking; τ, torsion; s, symmetric; as, antisymmetric; n.obs., not observed; n.i., not investigated. See Figure 1 for atom numbering and Table S4 for definition of symmetry coordinates. [b] Other observed bands, assigned to anharmonic vibrations: trans: 2767.2 (2x ν ring1), 2740.9 (ν ring3 + ν ring2), 1719.3 (γ(C−H10/11)$_s$ + δ ring2), 1605.3 (2x γ(C−H9)), 1550.9 (γ(C−H9) + γ(C−H10/11)$_s$), 1342.4 (δ(C=O) + τ ring2), 1196.8 (2x τ ring2), 1176.0 (γ(C−H10/11) + γ (C6−C3)) and 1174.5 (δ ring1 + γ (C6−C3)); cis: 2805.7 (ν ring3 + δ(C−H11)), 2756.8 (?), 1585.4 (γ(C−H10/11)$_{as}$ + (γ(C−H10/11)$_s$), 1200.0 (2x τ ring2). [c] B3LYP/6-311++G(d,p) calculated wavenumbers were scaled by 0.978; values in parentheses are calculated IR intensities (in km mol^{-1}).

experimental estimate obtained by Marstokk and Møllendal from the analysis of the microwave spectrum of 3FA.[29]

Irradiations of the samples carried out using UV light filtered by bandpass filters transmitting at λ > 375, 337, and 283 nm were found not to induce any substantial changes in the observed experimental spectra. However, changes started to occur promptly when the sample was irradiated with λ > 234 nm. These photoinduced changes could be easily interpreted as the trans → cis photoinduced isomerization reaction. The reliability of this interpretation is based on the fact that the bands due to both trans and cis conformers were present in the spectrum of the initially deposited matrix. As a result of irradiation, one group of the bands (due to cis form) increased their intensity, whereas another group (trans) decreased and no new bands appeared (see Figure 5). This fact allowed for an easy identification of the bands ascribable to each conformer and strongly facilitated the assignments of the bands in the experimental spectra, which are presented in Table 3. Figure 6 shows the observed changes in the infrared spectrum of the matrix-isolated compound after 60 min of irradiation.

The progress of the changes with time of irradiation is shown in Figure 7. The figure demonstrates that the observed isomer-ization kinetics is well fitted by a single exponential decay for both conformers (correlation coefficients of ca. 0.999). The fitted time constants t_a for isomerizations of the two conformers are about 13 min and practically equal to each other, considering the accuracy of the fits. The starting amounts of the conformers are equal to 88% (trans) and 12% (cis) and correspond to the equilibrium populations in the gas phase at room temperature. The asymptotic limits, corresponding to the fractional populations of the conformers in the photostationary state, are practically attained as fast as after one hour of irradiation. Such photochemical behavior is very similar to what was recently observed for pyrrole-2-carbaldehyde.[47] The sum of the two asymptotic values 62.2% (trans) and 36.6% (cis) shows that there is practically no loss of 3FA in the process of the photoisomerization induced by UV light with λ > 234 nm. Finally, we shall note that the photostationary state obtained under these conditions is characterized by the trans/cis population ratio of ~1.85.

To get further details on the mechanism of the photoisomerization, TD-DFT (B3LYP) calculations were carried out. The results of these calculations are summarized in Table 4 and Figure 8.
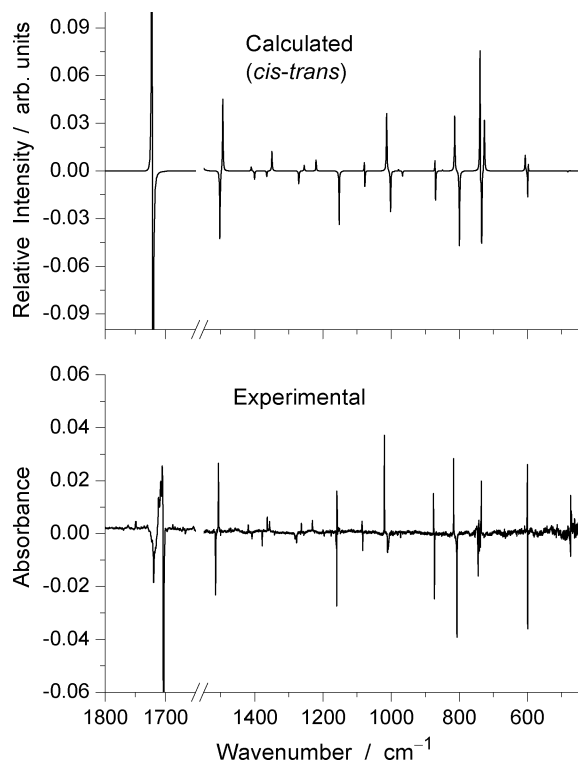
Figure 6. Bottom: difference infrared spectrum (irradiated matrix by UV light, $\lambda > 234$ nm for 60 min *minus* as-deposited matrix) of 3FA, showing the trans → cis photoisomerization. Negative absorbance corresponds to decreasing bands of the initially present trans form. Positive peaks correspond to growing absorptions due to the photo-produced cis conformer (also initially present). Top: Simulated cis−trans difference spectrum based on the B3LYP/6-311++G(d,p) calculated infrared spectra of the two 3FA conformers. Note that the bands in the 1800−1660 cm^{-1} region are truncated.

Analysis of Table 4 shows that, among the excitations accessible when irradiation is performed with $\lambda > 234$ nm (5.30 eV), that is, to S_1 and S_2 states, only excitation to S_2 has substantial oscillator strength. Direct $S_0 \rightarrow S_1$ excitation has nπ* character, and although it is not strictly forbidden, it should be very ineffective due to the very low value of the oscillator strength. Indeed, as mentioned previously, the irradiation with $\lambda > 283$ nm was inefficient in promoting any conformational isomerization process. Since $\lambda = 283$ nm corresponds to ∼4.4 eV, the energy of the corresponding UV excitation is below S_2, however it is well above S_1. This is an additional indication that the observed photochemical changes should be promoted by the excitation to S_2.

The potential energy profiles of the excited states calculated as a function of the aldehyde group rotation (see Figure 8) show that all of S_1, S_2, and S_3 states have a minimum at the cis conformation, which is, in those states, more stable than the trans conformation by 6.3, 17.0, and 10.5 kJ mol^{-1}, respectively. In S_1, cis and trans conformations correspond to the two minima, which are separated by a high energy barrier (cis → trans: 60.0 kJ mol^{-1}; 53.7 kJ mol^{-1} in the reverse direction). On the other hand, the bright S_2 state shows 3 minima: at the cis, trans, and perpendicular conformations. Refinement of the potential energy S_2 surface around the value of 90° revealed a minimum at ∼97° (96.73°; 4.7199 eV, global minimum).

The calculated $\Delta E_{\text{trans}-(\sim97°)}$ and $\Delta E_{\text{cis}-(\sim97°)}$ values amount to 19.2 and 2.2 kJ mol^{-1}, respectively. The trans → (∼97°) barrier is very small, 5.1 kJ mol^{-1}, whereas that separating the cis form from the ∼97° minimum is much larger: 25.2 kJ mol^{-1}.
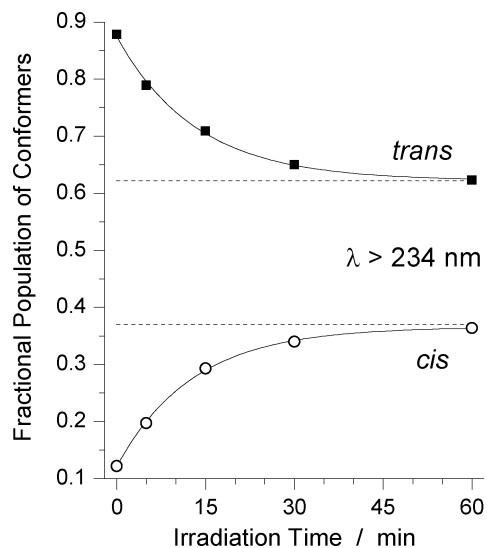

Figure 7. Kinetics of conformational changes with the time of irradiation ($\lambda > 234$ nm) estimated from the dependence of the intensities of selected characteristic bands of trans (871.6/872.7 and 806.8 cm^{-1}) and cis (875.6 and 816.6 cm^{-1}) conformers. The integrated experimental band intensities were reduced by the corresponding calculated intensities. Solid lines: exponential fits according to the equation [$y = A \exp(-x/t_a) + y_0$]. Dashed lines: asymptotic limits (y_0). The fitted equations for the changes in the fractional populations of the trans (black squares) and cis (white circles) forms are defined by the following (A, t_a, y_0) parameters. Trans: (0.253 ± 0.008, 13.4 ± 1.1, 0.622 ± 0.006; R^2= 0.9983); cis: (−0.245 ± 0.004, 12.8 ± 0.6, 0.366 ± 0.003; R^2= 0.9994).

TABLE 4: Energy of Vertical Absorption (ΔE) and Oscillator Strength (f) of Trans and Cis Conformers of 3FA Calculated for their Ground State Equilibrium Geometries Using the TD-DFT Method at the B3LYP/6-311++G(d,p) Level

	trans 3FA				cis 3FA		
state	type	ΔE (eV)	f	state	type	ΔE (eV)	f
S_0 (A')		0.00		S_0 (A')		0.046	
S_1 (A'')	nπ*	3.91	0.0002	S_1 (A'')	nπ*	3.79	0.0002
S_2 (A')	$\pi\pi$*	4.92	0.0574	S_2 (A')	$\pi\pi$*	4.70	0.0438
S_3 (A')	$\pi\pi$*	6.01	0.1524	S_3 (A')	$\pi\pi$*	5.85	0.1114
T_1 (A'')		3.32		T_1 (A')		3.14	
T_2 (A')		3.38		T_2 (A'')		3.24	
T_3 (A')		4.36		T_3 (A')		4.43	
T_4 (A')		4.78		T_4 (A')		4.77	
T_5 (A')		5.78		T_5 (A')		5.83	
T_6 (A'')		5.93		T_6 (A')		6.05	

The format of the S_2 potential energy profile for rotation of the aldehyde group in 3FA can easily explain the observed change in the conformational population taking place when the matrix-isolated compound was irradiated with $\lambda > 234$ nm. Indeed, excitation of both conformers with $\lambda > 234$ nm provides the excess energy of around 5.3 eV, which is well above all the barriers on the S_2 surface and can be followed by fast internal rotation in the S_2 excited state to the ∼97° minimum. Relaxation of S_2 from the ∼97° minimum can then produce either cis or trans ground state conformers by internal rotation in S_0. The experimentally observed conformational trans/cis ratio of ∼1.85, characteristic of the photostationary state, provides evidence that the probability of the relaxation of the excited 3FA molecule into the trans ground state conformation is higher. This prevalence of the trans form in the photostationary state can be explained by two factors: (i) the torsional coordinate at the minimum in S_2 equals ∼97° (see Figure 8), that is, the starting

12434 *J. Phys. Chem. A, Vol. 114, No. 47, 2010*
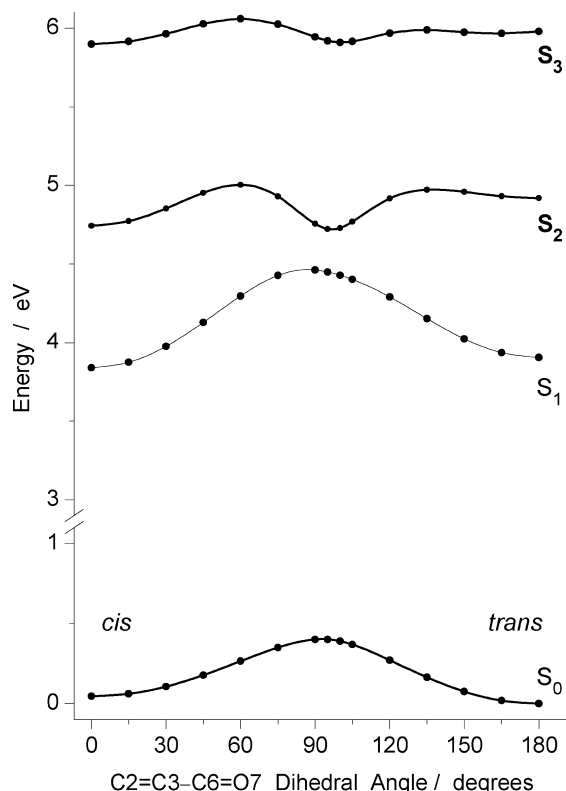
Kuş et al.

Figure 8. TD-DFT profiles of the lowest energy singlet states of 3FA calculated at the B3LYP/6-311++G(d,p) level of theory as functions of the internal rotation of the aldehyde group. Note ordinate break.

Figure 9. Bottom: difference spectrum (matrix irradiated with $\lambda >$ 200 nm) *minus* (matrix irradiated with $\lambda >$ 234 nm); positive bands correspond to photolysis products; negative bands are due to 3FA; asterisk indicates bands due to traces of water impurity present in the initial sample. Top: calculated stick spectra of 3FA photolysis products: furan (white squares), cyclopropene (black triangles), propadiene (black squares) and cyclopropene-3-carbaldehyde (white triangles). The calculated B3LYP/6-311++G(d,p) frequencies were scaled by 0.978); theoretical intensities of cyclopropene-3-carbaldehyde were multiplied by a factor of 0.5 in order to improve the concordance between the experimental and simulated spectrum. The calculated bands having intensities less than 1 km mol^{-1} are not shown (for all species).

position before relaxation is shifted in the direction of trans conformer; and (ii) the excitation energy of the cis conformer is lower than that of the trans, thus cis should be more easily excited and more quickly consumed.

It is also interesting to note that the calculated profile for internal rotation of the aldehyde group in S_3 is similar to that of S_2. The "perpendicular" S_3 minimum is shifted in the direction of the trans 3FA conformer even further and has the dihedral C=C—C=O angle of ~100° (100.4°; 5.9086 eV). Thus, conformational isomerization in 3FA should follow a similar pattern also in case of involvement of the S_3 state in the process (in S_3, the calculated $\Delta E_{trans-(\sim100°)}$ and $\Delta E_{(\sim100°)-cis}$ values are 5.6 and 1.0 kJ mol^{-1}, respectively, and the trans → (~100°) and cis → (~100°) barriers are 2.2 and 15.5 kJ mol^{-1}).

Photolysis of Matrix-Isolated 3FA. Prolonged irradiation of matrix-isolated 3FA with $\lambda >$ 200 nm light led to decrease of intensities of the infrared bands due to both trans and cis conformers. Simultaneously, new sets of bands emerged, which represent features due to products of photolysis of the compound.

Aromatic aldehydes have been shown to be able to undergo easy photodecarbonylation.[48-53] Benzaldehyde, *p*-anisaldehyde, and pyrrol-2-carbaldehyde isolated in argon matrices, for example, were found to decarbonylate, leading to formation of benzene, anisole, and pyrrole.[49-53] The photochemistry of 2-furaldehyde (2FA) in gas phase is also characterized by the ejection of carbon monoxide, according to two main photoprocesses yielding furane + CO and C_3H_4 + 2CO, respectively.[48] Evidence has been presented[48] that the latter process proceeds through an excited triplet molecule of furan as an intermediate. The observed C_3H_4 species resulting from the photolysis of 2FA were propyne, cyclopropene, and propadiene.[48] In the case of unsubstituted furan, a multitude of different photoproducts have been reported, either in the gas phase, liquid compound, or
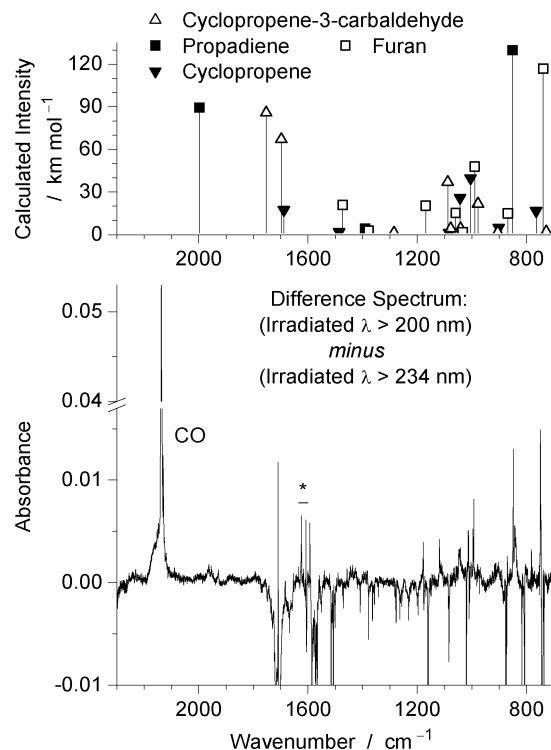
matrix-isolated compound.[48,54,55] These include not only CO and the products resulting from decarbonylation (propyne, cyclopropene, and propadiene), but also other products resulting from photoinduced isomerization processes: cyclopropene-3-carbaldehyde, vinylketene, 2,3-butadienal, and the Dewar furan.[54,56] Very interestingly, singlet furan has been found not to give rise to cyclopropene, whereas triplet sensitized furan produces cyclopropene as one of its main photoproducts.[48] Observation of cyclopropene is then a mark of involvement of triplet states in the photofragmentation of furan.

In the case of 3FA, we were able to identify in the photolyzed matrix the presence of CO, furan, cyclopropene-3-carbaldehyde, cyclopropene, and propadiene, which points to a very similar photochemistry of 3FA and 2FA (among the photoproducts of 2FA reported in ref 48, only propyne could not be affirmatively observed in the present study, although its production as a minor product or its initial photoproduction followed by fast isomerization to any other of the C_3H_4 observed species could not be excluded as well). Observation of cyclopropene, in particular, points to the involvement of a triplet state in the photolysis mechanism. Noteworthy is also the observation of the cyclopropene-3-carbaldehyde intermediate, which was also postulated to be involved in the photochemistry of 2FA.[48] The observed bands of the 3FA photoproducts are collected in Table S7. The assignments were made taking into account literature data for these species isolated in argon matrices[54,57-60] and also results of calculations made in the present study at the B3LYP/6-
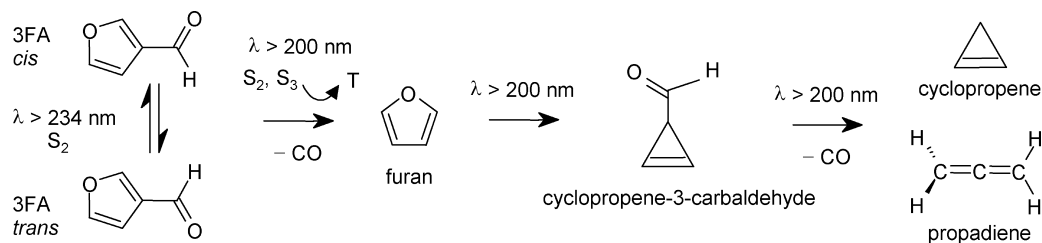
Figure 10. Summary of the photochemical reactions observed for matrix-isolated 3FA upon irradiation with $\lambda > 234$ nm and $\lambda > 200$ nm. T refers to the triplet manifold.

311G++(d,p) level. The most characteristic bands were observed: for furan at 1179.7/1177.7, 995.6/992.8, 748.5/746.7 and 603.3/602.3 cm^{-1}, corresponding to the νC$-$O as, δC$-$H, all-in-phase γC$-$H and δ-ring (butterfly) modes (bands appear as doublets due to existence of two different matrix sites for furan); for cyclopropene-3-carbaldehyde at 1709.8, 1696.1, and 1118.4 cm^{-1} (νC=O, νC=C and ν(C$-$C) s); for cyclopropene at 2980.8, 2904.9, 1012.3, and 585.2/580.0 cm^{-1} (νCH$_2$ as, νCH$_2$ s, δ(=CH) as and γ(=CH) s); and for propadiene in the 1967$-$1957 cm^{-1} region and at ca. 850 cm^{-1} (νC=C=C as and wCH$_2$) (see also Figure 9). The characteristic absorptions due to CO are observed in the 2120$-$2140 cm^{-1} range: the most intense band at 2138 cm^{-1} corresponds to weakly interacting or well-isolated monomeric CO, whereas the lower intensity bands indicate that part of the CO molecules did not diffuse from the original cage where they were formed and interact with other species resulting from fragmentation of 3FA.

Figure 10 summarizes the observed photoinduced processes. According to the proposed scheme, the photolysis mechanism in 3FA closely follows that previously proposed for 2FA.[48] The excitation energy used ($\lambda > 200$ nm) allows for efficient excitation of both S$_2$ and S$_3$ states (as already mentioned, the oscillator strength of S$_1$ is very small; Table 4). However, these two states clearly show different reactivity. In fact, the experimental results indicate that intersystem crossing from S$_2$ to the triplet manifold must be quite inefficient, since excitation at $\lambda > 234$ nm (S$_2$) led only (or practically only) to conformational isomerization, until the photostationary state associated with this process was achieved, and this takes place in the singlet manifold. On the other hand, irradiation with $\lambda > 200$ nm (both S$_2$ and S$_3$) led to photolysis, which involves the triplet state of the compound. Hence, it implies that the intersystem crossing from S$_3$ is quite effective. Indeed, the TD-DFT calculations predicted existence of 6 triplet states at energies below or about that of S$_3$; see Table 4. Once the triplet 3FA molecules are formed, the molecule decarbonylates forming triplet furan, which can either relax to the ground state or undergo subsequent decarbonylation reactions to form propadiene or cyclopropene. According to the previous studies,[48,54-56] cyclopropene-3-carbaldehyde should be an intermediate in these latter processes and, in the present study, it was indeed observed experimentally.

Conclusions

The photorotamerization and photodecomposition of matrix-isolated 3-furaldehyde (3FA) was studied using FTIR spectroscopy and quantum chemical methods. The trans conformer of the molecule was calculated to be the most stable form in the ground electronic state, being more stable than the cis conformer by ca. 4 kJ mol^{-1}. The relative stability of the two conformers was explained using the NBO method. The barrier to conformational isomerization in S$_0$ was calculated as being ca. 34 kJ mol^{-1} (trans-to-cis). In fair agreement with their calculated

relative energies and the high barrier of rotamerization, the trans and cis conformers were trapped in an argon matrix from the compound room temperature gas phase in the proportion $\sim$7:1. The IR spectrum of each conformer was extracted from the experimentally observed spectrum and fully assigned with help of the theoretically calculated spectra.

Broad-band UV-irradiation ($\lambda > 234$ nm) of the matrix-isolated compound resulted in partial trans $\rightarrow$ cis isomerization, which ended at a photostationary state with the trans/cis ratio being $\sim$1.85:1. This result was interpreted based on results of time-dependent DFT (B3LYP)/6-311++G(d,p) calculations. In particular, it was shown that the bright state corresponds to S$_2$, which exhibits 3 minima (at cis, trans, and $\sim$97° geometries of the aldehyde group). Relaxation of the S$_2$ state from the $\sim$97° minimum can then produce either cis or trans ground state conformers by internal rotation in S$_0$, leading to the photostationary state where the population is shifted in favor of the trans conformer when the matrix isolated compound was irradiated with $\lambda > 234$ nm.

Irradiation at higher energies ($\lambda > 200$ nm; S$_2$ and S$_3$) of the matrix-isolated 3FA led to decarbonylation of the compound, yielding furan, cyclopropene-3-carbaldehyde and two C$_3$H$_4$ isomers (cyclopropene and propadiene), in a process that seems to be very similar to that reported previously for the analogous compound 2FA.[48] In particular, observation of cyclopropene as one of the main products of photolysis indicates that this involves triplet furan as intermediate.

Supporting Information Available: Table S1, with DFT-(B3LYP)/6-311++G(d,p) optimized geometries for trans and cis conformers of 3FA; Tables S2 and S3, with NBOs for trans and cis conformers of 3FA, respectively; Table S4, with definition of internal coordinates used in the normal-mode analysis calculations; Tables S5 and S6, with results of normal-mode analysis for trans and cis conformers of 3FA, respectively; Table S7, with assignments of bands due to the observed photoproducts of 3FA. This material is available free of charge via Internet at http://pubs.acs.org.

References and Notes

(1) Yokelson, R. J.; Karl, T.; Artaxo, P.; Blake, D. R.; Christian, T. J.; Griffith, D. W. T.; Guenther, A.; Hao, W. M. *Atmos. Chem. Phys.* **2007**, *7*, 5175–5196.

(2) Karl, T. G.; Christian, T. J.; Yokelson, R. J.; Artaxo, P.; Hao, W. M.; Guenther, A. *Atmos. Chem. Phys.* **2007**, *7*, 5883–5897.

(3) Amaro, M. I.; Monasterios, M.; Avendaño, M.; Charris, J. J. *J. Appl. Tox.* **2009**, *29*, 36–41.

(4) Seawright, A. A.; Mattocks, A. R. *Experientia* **1973**, *29*, 1197–1200.

(5) Bell, J. U. *Waste Manage.* **2002**, *22*, 405–412.

12436 *J. Phys. Chem. A, Vol. 114, No. 47, 2010*

Kuş et al.

(6) Spano, N.; Ciulu, M.; Floris, I.; Panzanelli, A.; Pilo, M. I.; Piu, P. C.; Salis, S.; Sanna, G. *Talanta* **2009**, *78*, 310–314.

(7) Park, D.; Maga, J. A. *Food Chem.* **2006**, *99*, 538–545.

(8) Cabañas, B.; Tapia, A.; Villanueva, F.; Salgado, S.; Monedero, E.; Martín, P. *Int. J. Chem. Kinetics* **2008**, *40*, 670–678.

(9) Gilman, H.; Burtner, R. R. *J. Am. Chem. Soc.* **1932**, *54*, 3014.

(10) Roques, B. P.; Combrisson, S. *Can. J. Chem.* **1973**, *51*, 573–581.

(11) John, I. G.; Radom, L. *J. Am. Chem. Soc.* **1978**, *100*, 3981–3991.

(12) John, I. G.; Ritchie, G. L. D.; Radom, L. *J. Chem. Soc.: Perkin Trans. 2* **1977**, *1601*, 1607.

(13) Sheinker, V. N.; Garnovskii, A. D.; Osipov, O. A. *Russ. Chem. Rev.* **1981**, *50*, 336–352.

(14) Andrieu, C. G.; Chatain-Cathaud, C.; Fournié-Zaluski, M. C. *J. Mol. Struct.* **1974**, *22*, 433–444.

(15) Benassi, R.; Folli, U.; Mucci, A.; Schenetti, L.; Taddei, F. *Magn. Reson. Chem.* **1987**, *25*, 804–810.

(16) Benassi, R.; Folli, U.; Schenetti, L.; Taddei, F. *J. Chem. Soc.: Perkin Trans. 2* **1988**, *1501*, 1507.

(17) Volka, K.; Adámek, P.; Stibor, I.; Ksandr, Z. *J. Radioanal. Chem.* **1976**, *30*, 205–214.

(18) Hofmann, H. J.; Birner, P. *Chem. Phys. Lett.* **1976**, *37*, 608–610.

(19) Abraham, R. J.; Siverns, T. M. *Tetrahedron* **1972**, *28*, 3015–3024.

(20) Little, T. S.; Qiu, J.; Durig, J. R. *Spectrochim. Acta, Part A* **1989**, *45*, 789–794.

(21) Ashish, H.; Ramasami, P. *Mol. Phys.* **2008**, *106*, 175–185.

(22) Crespo-Otero, R.; Montero, L. A.; Rosquete, G.; Padrón-García, J. A.; González-Jonte, R. H. *J. Comput. Chem.* **2004**, *25*, 429–438.

(23) Montero, L. A.; González-Jonte, R.; Díaz, L. A.; Alvarez-Idaboy, J. R. *J. Phys. Chem.* **1994**, *98*, 5607–5613.

(24) Mönnig, F.; Dreizler, H.; Rudolph, H. D. *Z. Naturforsch., Part A* **1965**, *A 20*, 1323.

(25) Klapstein, D.; MacPherson, C. D.; O'Brien, R. T. *Can. J. Chem.* **1990**, *68*, 747–754.

(26) Baldridge, K. K.; Jonas, V.; Bain, A. D. *J. Chem. Phys.* **2000**, *113*, 7519–7529.

(27) Miller, F. A.; Fateley, W. G.; Witkowski, R. E. *Spectrochim. Acta, Part A* **1967**, *A 23*, 891–908.

(28) Rogojerov, M.; Keresztury, G.; Jordanov, B. *Spectrochim. Acta, Part A* **2005**, *61*, 1661–1670.

(29) Marstokk, K.-M.; Møllendal, H. *Acta Chem. Scand.* **1992**, *46*, 923–927.

(30) Liégeois, C.; Barker, J. M.; Lumbroso, H. *Bull. Soc. Chim. Fr., Part I* **1978**, *329*, 332.

(31) Lunazzi, L.; Placucci, G.; Macciantelli, D. *Tetrahedron* **1991**, *47*, 6427–6434.

(32) Gacel, G.; Fournié-Zaluski, M. C.; Roques, B. P. *Org. Magn. Reson.* **1976**, *8*, 525–529.

(33) Andrzejewska, A.; Lapinski, L.; Reva, I.; Fausto, R. *Phys. Chem. Chem. Phys.* **2002**, *4*, 3289–3296.

(34) Frisch, M. J.; Trucks, G. W.; Schlegel, H. B.; Scuseria, G. E.; Robb, M. A.; Cheeseman, J. R.; Montgomery, Jr., J. A.; Vreven, T.; Kudin, K. N.; Burant, J. C.; Millam, J. M.; Iyengar, S. S.; Tomasi, J.; Barone, V.; Mennucci, B.; Cossi, M.; Scalmani, G.; Rega, N.; Petersson, G. A.; Nakatsuji, H.; Hada, M.; Ehara, M.; Toyota, K.; Fukuda, R.; Hasegawa, J.; Ishida, M.; Nakajima, T.; Honda, Y.; Kitao, O.; Nakai, H.; Klene, M.; Li, X.; Knox, J. E.; Hratchian, H. P.; Cross, J. B.; Bakken, V.; Adamo, C.; Jaramillo, J.; Gomperts, R.; Stratmann, R. E.; Yazyev, O.; Austin, A. J.; Cammi, R.; Pomelli, C.; Ochterski, J. W.; Ayala, P. Y.; Morokuma, K.; Voth, G. A.; Salvador, P.; Dannenberg, J. J.; Zakrzewski, V. G.; Dapprich, S.; Daniels, A. D.; Strain, M. C.; Farkas, O.; Malick, D. K.; Rabuck, A. D.; Raghavachari, K.; Foresman, J. B.; Ortiz, J. V.; Cui, Q.; Baboul, A. G.; Clifford, S.; Cioslowski, J.; Stefanov, B. B.; Liu, G.; Liashenko, A.; Piskorz, P.; Komaromi, I.; Martin, R. L.; Fox, D. J.; Keith, T.; Al-Laham, M. A.; Peng, C. Y.; Nanayakkara, A.; Challacombe, M.; Gill, P. M. W.; Johnson, B.; Chen, W.; Wong, M. W.; Gonzalez, C.; Pople, J. A. *Gaussian 03, Revision C.02*; Gaussian, Inc.: Wallingford CT, 2004.

(35) Frisch, M. J.; Pople, J. A.; Binkley, J. S. *J. Chem. Phys.* **1984**, *80*, 3265–3269.

(36) Clark, T.; Chandrasekhar, J.; Spitznagel, G. W.; Schleyer, P. v. R. *J. Comput. Chem.* **1983**, *4*, 294–301.

(37) Becke, A. D. *Phys. Rev. A* **1988**, *38*, 3098–3100.

(38) Lee, C. T.; Yang, W. T.; Parr, R. G. *Phys. Rev. B* **1988**, *37*, 785–789.

(39) Bauernschmitt, R.; Ahlrichs, R. *Chem. Phys. Lett.* **1996**, *256*, 454–464.

(40) Stratmann, R. E.; Scuseria, G. E.; Frisch, M. J. *J. Chem. Phys.* **1998**, *109*, 8218–8224.

(41) Reed, A. E.; Curtiss, L. A.; Weinhold, F. *Chem. Rev.* **1988**, *88*, 899–926.

(42) Weinhold, F.; Landis, C. R. *Valency and Bonding. A Natural Bond Orbital Donor-Acceptor Perspective*; Cambridge University Press: New York., 2005.

(43) Schachtschneider, J. H.; Mortimer, F. S. *Vibrational Analysis of Polyatomic Molecules. VI. FORTRAN IV Programs for Solving the Vibrational Secular Equation and for the Least-Squares Refinement of Force Constants. Project No. 31450. Structural Interpretation of Spectra*; Shell Development Co.: 1969.

(44) Pulay, P.; Fogarasi, G.; Pang, F.; Boggs, J. E. *J. Am. Chem. Soc.* **1979**, *101*, 2550–2560.

(45) Fausto, R.; Batista de Carvalho, L. A. E.; Teixeira-Dias, J. J. C.; Ramos, M. N. *J. Chem. Soc., Faraday Trans. 2* **1989**, *85*, 1945–1962.

(46) McKean, D. C. *Chem. Soc. Rev.* **1978**, *7*, 399–422.

(47) Castiglioni, C.; Gussoni, M.; Zerbi, G. *J. Chem. Phys.* **1985**, *82*, 3534–3542.

(48) Hiraoka, H.; Srinivasan, R. *J. Chem. Phys.* **1968**, *48*, 2185–2189.

(49) Kuş, N.; Sharma, A.; Reva, I.; Lapinski, L.; Fausto, R. *J. Phys. Chem. A* **2010**, *114*, 7716–7724.

(50) Giuliano, B. M.; Reva, I.; Fausto, R. *J. Phys. Chem. A* **2010**, *114*, 2506–2517.

(51) Silva, C. R.; Reilly, J. P. *J. Phys. Chem. A* **1997**, *101*, 7934–7942.

(52) Yang, J. J.; Gobeli, D. A.; El-Sayed, M. A. *J. Phys. Chem.* **1985**, *89*, 3426–3429.

(53) Brühlmann, U.; Nonella, M.; Russegger, P.; Huber, J. R. *Chem. Phys.* **1983**, *81*, 439–447.

(54) Rendall, W. A.; Clement, A.; Torres, M.; Strausz, O. P. *J. Am. Chem. Soc.* **1986**, *108*, 1691–1692.

(55) Srinivasan, R. *J. Am. Chem. Soc.* **1967**, *89*, 1758.

(56) D'Auria, M. *Adv. Heterocycl. Chem.* **2001**, *79*, 41–88.

(57) Sánchez-García, E.; Mardyukov, A.; Tekin, A.; Crespo-Otero, R.; Montero, L. A.; Sander, W.; Jansen, G. *Chem. Phys.* **2008**, *343*, 168–185.

(58) Sánchez-García, E.; Mardyukov, A.; Studentkowski, M.; Montero, L. A.; Sander, W. *J. Phys. Chem. A* **2006**, *110*, 13775–13785.

(59) Maier, G.; Lautz, C.; Senger, S. *Chem.—Eur. J.* **2000**, *6*, 1467–1473.

(60) Ball, D. W.; Pong, R. G. S.; Kafafi, Z. H. *J. Am. Chem. Soc.* **1993**, *115*, 2864–2870.